

Dynamic Subchannel Grouping Algorithm using Local Gateways for Enterprise Small-cell Networks[☆]

김 세 진^{1*}
Se-Jin Kim

ABSTRACT

In this paper, we propose a novel dynamic subchannel grouping (DSG) algorithm to maximize the system capacity considering intended proper outage probability for the downlink of enterprise small-cell networks (ESNs). In the proposed DSG scheme, a local gateway (LGW) which is installed in a building dynamically divides the frequency bandwidth into different numbers of subchannel groups (SGs) based on the numbers of small-cell access points (SAPs) and small-cell user equipments (SUEs) per floor. Then, the LGW assigns the SGs to SAPs and the SAPs allocate them to their serving SUEs. Through simulation results, we show that the proposed DSG scheme is appropriate for the ESNs compared to the conventional small-cell networks in which all SAPs use the number of fixed SGs in terms of the system capacity and outage probability.

☞ keyword : Small-cell networks, Enterprise, Local gateway, Dynamic, Subchannel grouping

1. Introduction

Recent technological advances in mobile devices, e.g., smart phones, tablet PCs, and so on, have led to increase wireless data traffic explosively [1][2][3]. Further, more than half of the traffic occur indoor environment during daytime [4] and small-cell networks have become an attractive solution to extend the coverage of conventional cellular networks (CCNs) with providing high speed data service [5][6][7][8][9]. Thus, the world's major mobile network operators (MNOs) currently show a great deal of attention to adopt small-cells for the enterprise environments, i.e., enterprise small-cell networks (ESNs), because a lot of people work in their companies during daytime and it means that ESNs are more useful than residential small-cell networks (RSNs) in which one or two small-cell access

points (SAPs) are installed in each detached house [10][11][12][13][14]. However, in ESNs, a lot of SAPs are densely installed in a building and they serve different numbers of small-cell user equipments (SUEs) with strong interference from neighbor SAPs. Most work have been studied about small-cell networks are for RSNs and a couple of work have been studied for ESNs [15][16]. In [15], authors proposed a load sharing scheme using a handover margin and transmit power managements based on fuzzy logic controller. On the other hand, in [16], authors proposed an adaptive sub-band allocation scheme based on the interference graph. However, both schemes in [15] and [16] use distributed methods and thus every SAP needs to check the traffic load and interference of adjacent SAPs to use those schemes.

In this paper, we propose a novel dynamic subchannel grouping (DSG) algorithm to maximize the system capacity considering intended proper outage probability for the downlink (DL) of ESNs. In the proposed DSG scheme, a local gateway (LGW) which is installed in a building dynamically divides the frequency bandwidth into different numbers of subchannel groups (SGs) based on the numbers of SAPs and SUEs per floor. Then, the LGW assigns the SGs to SAPs and the SAPs allocate them to their serving

¹ Dept. of Computer Science and Statistics, Chosun University, Gwangju 61452, Korea.

* Corresponding author (sjkim@chosun.ac.kr)

[Received 5 August 2017, Reviewed 14 August 2017(11 October 2017), Accepted 1 November 2017]

☆ This work was supported by the National Research Foundation of Korea (NRF) Grant funded by the Korean Government (MSIP) (No. 2015R1C1A1A01055869).

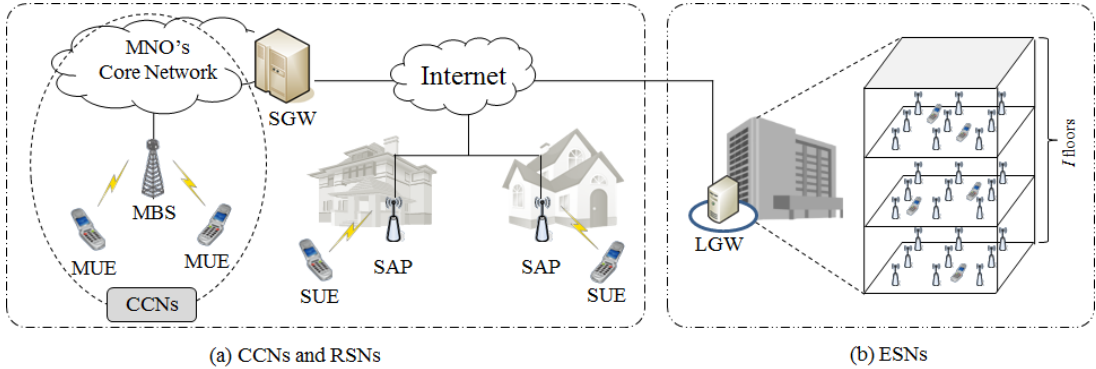


(Figure 1) System architectures of RSNs and ESNs

SUEs. Through simulation results, we show that the proposed DSG scheme is appropriate for the ESNs compared to the conventional small-cell networks in which all SAPs use the number of fixed SGs in terms of the system capacity and outage probability.

The remainder of this paper is organized as follows. Section 2 introduces various system models and Section 3 explains the proposed DSG scheme using the LGW. Then, Section 4 evaluates the system performance and section 5 concludes this paper with future research direction.

2. System Model

2.1 System architectures for ESNs

Fig. 1 shows system architectures of RSNs and ESNs [10][11]. As shown in Fig. 1-(a), the RSN consists of SAPs, SUEs, and a small-cell gateway (SGW) and they are added to the CCN that has two components, i.e., macro base stations (MBSs) and macro user equipments (MUEs). Further, all SAPs are connected to the MNO's core network through the Internet and SGW and then the SGW manages all SAPs for the initial configuration, channel allocation, handover, and so on. However, each SGW manages up to 1000 SAPs and thus the architecture is appropriate for RSNs since each detached house has one or more SAPs in RSNs. On the other hand, as shown in Fig. 1-(b), in ESNs, a lot of SAPs and SUEs are deployed in a building and a LGW is added to the architecture of ESNs to manage the SAPs and

SUEs instead of the SGW with low transmission delay [17]. That is, the LGW dynamically assigns SGs to SAPs based on the numbers of SAPs and SUEs.

Small-cell networks consider two kinds of bandwidth allocation schemes, i.e., shared reuse and split reuse [18]. In the shared reuse scheme, the total frequency bandwidth, B_{Total} , is used by both MUEs and SUEs at the same time while in the split reuse scheme, B_{Total} is divided into two groups for the macrocell and small-cell networks, B_{MC} , and B_{SC} , and thus there is no interference between MBSs and SAPs. In this paper, we use the split reuse scheme because the shared reuse scheme has different performance results according to the distance between the MBS and buildings with ESNs. Further, for ESNs, we consider a square topology of each floor and the width of the building is $W_{Building}$ while the number of total floors in a building is I and the height of each floor is H_{Floor} . The gap between floors and the height of SAPs are H_{Gap} and H_{SAP} , respectively. In each floor, J SAPs are installed in grid patterns and K SUEs are uniformly distributed. The SGW and LGW divide B_{SC} into N SGs and send this information to SAPs in RSNs and ESNs, respectively. Then, the SAP randomly allocates different SGs to their serving SUEs (one SG to one SUE).

2.2 Channel and SINR models

We consider a path loss model between the SAP and SUE, PL , as shown in (1).

$$PL = \begin{cases} \alpha + \beta & \text{for the same floor} \\ \max(\alpha, \delta) + \beta & \text{for different floors,} \end{cases} \quad (1)$$

where, $\alpha = 38.46 + 20 \cdot \log_{10} R$ and R is the distance between the SAP and SUE. $\beta = 0.7d_{2D,in}$ for the same floor while $\beta = 0.7d_{2D,in} + 18.3 \cdot b^{((b+2)/(b+1)-0.46)}$ for different floors where b is the number of penetrated floors between SAPs and SUEs, the term $0.7d_{2D,in}$ takes account of penetration loss due to walls inside a building and $\delta = 15.3 + 37.6 \cdot \log_{10} R$ [17].

The signal to interference plus noise ratio (SINR) model is defined as the ratio of signal power to interference power. Let $\gamma_{SUE_{i,j,k}}^n$ be the SINR of the k -th SUE ($1 \leq k \leq K$) serviced by the j -th SAP ($1 \leq j \leq J$) on the i -th floor ($1 \leq i \leq I$) for the n -th SG ($1 \leq n \leq N$). Then, $\gamma_{SUE_{i,j,k}}^n$ can be expressed as (2).

$$\gamma_{SUE_{i,j,k}}^n = \frac{R_{SAP_{i,j,k}}^n}{N_0 + \sum_{x=1}^I \sum_{\substack{y=1 \\ x \neq i | y \neq j}}^J I_{SAP_{x,y,k}}^n \cdot \psi_{x,y,k}^n}, \quad (2)$$

where, $R_{SAP_{i,j,k}}^n$ is the strength of the received signal of the k -th SUE served by the j -th SAP on the i -th floor for the n -th SG while $I_{SAP_{x,y,k}}^n$ is the strength of interfering signals to the k -th SUE from the y -th SAP ($1 \leq y \leq J$) on the x -th floor ($1 \leq x \leq I$) for the n -th SG. Further, N_0 is the white noise power and $\psi_{x,y,k}^n$ is a binary indicator, $\psi_{x,y,k}^n = 1$ if the y -th SAP on the x -th floor uses the n -th SG for the k -th SUE and 0 otherwise.

2.3 System capacity and outage probability

After obtaining $\gamma_{SUE_{i,j,k}}^n$, we can analyze the capacity of the k -th SUE served by the j -th SAP on the i -th floor, $C_{SUE_{i,j,k}}$, using the Shannon theorem as expressed in (3).

$$C_{SUE_{i,j,k}} = \left(\frac{B_{SC}}{N} \right) \log_2 \left(1 + \gamma_{SUE_{i,j,k}}^n \right). \quad (3)$$

Then, the capacity of all SAPs in the building, $C_{Building}$, and the average capacity of the SUE, $\overline{C_{SUE}}$, are calculated by (4) and (5), respectively.

$$C_{Building} = \sum_{i=1}^I \sum_{j=1}^J \sum_{k=1}^K \left(\frac{B_{SC}}{N} \right) \cdot \log_2 \left(1 + \gamma_{SUE_{i,j,k}}^n \right) \psi_{x,y,k}^n, \quad (4)$$

$$\overline{C_{SUE}} = \frac{C_{Building}}{IN}. \quad (5)$$

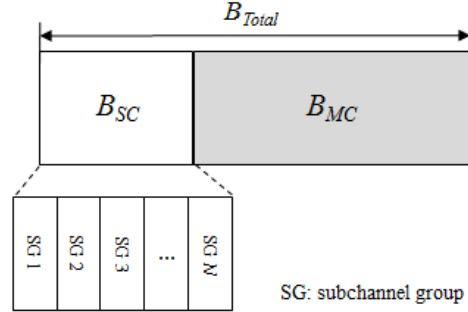


(Figure 2) N SGs in B_{SC} for the split reuse.

Further, we evaluate the outage probability for SUEs, P_{out} , as expressed in (6).

$$P_{out} \approx \frac{\eta_1 + \eta_2}{I \cdot K}, \quad (6)$$

where, η_1 and η_2 are the numbers of SUEs that have SINR values less than the SINR threshold, γ_{th} , and SUEs that receive no SG from their serving SAPs because the number of SUEs served by their SAPs is greater than the number of SGs, respectively.

3. Proposed DSG Scheme using the LGW

Fig. 2 shows the bandwidth allocation for the split reuse in small-cell networks. The SAPs use B_{SC} in B_{Total} for SUEs. In RSNs, the SGW divides B_{SC} into N SGs that are fixed, e.g., N is 5, 10, or 20 SGs. Thus, the number of SUEs that receive no SG from their serving SAPs can be increased as N decreases. On the other hand, in the proposed DSG scheme, the LGW knows the numbers of SAPs and SUEs in the building by exchanging control messages between the

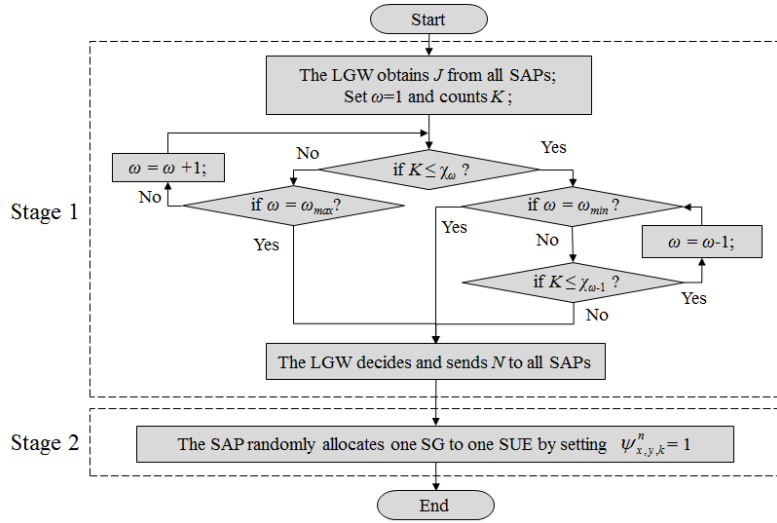


(Figure 3) A flow chart for the proposed DSG scheme using the LGW.

LGW and SAPs, periodically. Then, the LGW dynamically divides B_{SC} into different numbers of SGs, i.e., N is different based on the numbers of SAPs and SUEs per floor in the building of EFNs. Further, the amount of the frequency bandwidth per SG is depend on N , i.e., B_{SC} / N . That is, the amount of the frequency bandwidth per SG decreases as N increases and vice versa.

Fig. 3 shows a flow chart for the proposed DSG scheme using the LGW. The proposed DSG scheme consists of two stages. In stage 1, the LGW obtains J and counts K using control messages from all SAPs. Then, the LGW increases and decreases N when K becomes over and lower than the previously defined number of SUEs, χ_ω , respectively. Here, ω is the level between 1 and 5 for χ_ω . For example, the LGW increases ω based on J and K and then sends a control message with N to all SAPs to update when K exceeds the specific numbers of SUEs in χ_ω that are different according to J , i.e. 3×3 (9 SAPs) or 5×5 (25 SAPs) grid pattern. On the other hand, in stage 2, SAPs assign N SGs to their serving SUEs but the SAP randomly allocates one SG with $\lfloor B_{SC}/N \rfloor$ to one SUE. In other words, the serving SAP sets $\psi_{x,y,k}^n = 1$ when the y -th SAP on the x -th floor allocates the n -th SG for the k -th SUE. Table 1 shows N according to ω in the proposed DSG scheme.

(Table 1) N according to ω in the proposed DSG scheme

ω	χ_ω	N (3x3, J=9)	N (5x5, J=25)
1 (ω_{\min})	10	5	5
2	20	10	10
3	30	15	10
4	40	20	15
5 (ω_{\max})	50	25	15

4. Performance Evaluation

We investigate the DL performance of the proposed DSG scheme in terms of the system capacity, outage probability, and resource utilization for ESNs using a Monte Carlo simulation. We performed 200 independent simulations to evaluate the system performance according to the different numbers of SUEs, SAPs, and SGs in the analysis. We assume that the building with EFNs is open space such as department stores and business buildings and thus a log-normal shadow fading is considered with zero mean and standard deviation of 4dB for the link between the SAP and SUEs [17]. The values of noise figure for SUE is 8dB and $\gamma_{\min} = -6$ dB. Table 1 gives N according to ω in the proposed DSG scheme and each level is already defined considering intended proper outage probability less than the boundary of

(Table 2) System parameters

Parameter	Value
Carrier frequency	2GHz
B_{Total}, B_{SC}	20MHz, 5MHz
The number of floors (l)	10
The number of SAPs/floors (J)	9 (3x3), 25 (5x5)
The number of SUEs/floors (K)	10, 20, 30, 40, 50
The number of SGs (N)	RSN: 5, 10, 20 Prop. (3x3): 5~25 Prop. (5x5): 5~15
SAP Tx power	20dBm [17]
$W_{Building}$	50m
H_{floor}	3m
H_{Gap}	0.5m
H_{SAP}	3m
SINR threshold (γ_{th})	-6dB
Boundary of P_{out}	0.05
N_0	-174dBm/Hz

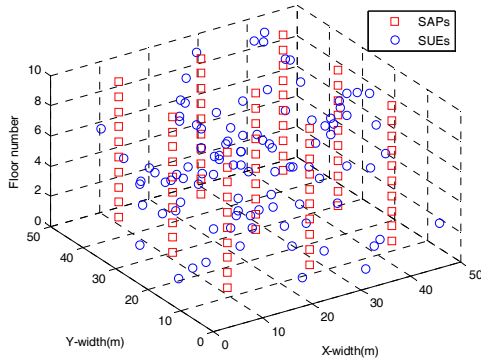


(Figure 4) An example of deployment of 9 SAPs with the 3x3 grid pattern and 10 SUEs per floor in a building

P_{out} . For example, the values of N are respectively 15 and 10 for the 3x3 and 5x5 grid pattern models in the proposed DSG scheme when $\omega=3$, i.e., $\chi_\omega=30$. Table 2 gives the key system parameters and Fig. 4 shows an example of deployment of 9 SAPs with the 3x3 grid pattern and 10 SUEs per floor in a building.

Fig. 5 describes the results of $\overline{C_{SUE}}$ as the number of SUEs increases with different N . In both schemes, the capacity results decrease as K increases and the 5x5 grid pattern model has better performance than the 3x3 grid

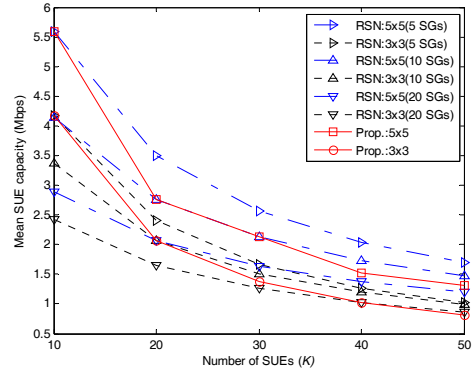


(Figure 5) Average capacity of SUE

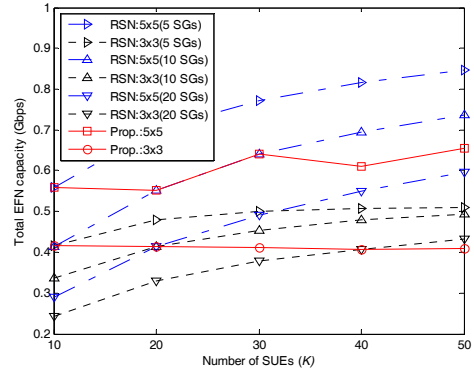


(Figure 6) Total capacity of SUEs in a building

pattern model because the 5x5 grid pattern model can use more SGs with 25 SAPs. Also, the capacity results decrease as N increases. The reason is that the amount of frequency bandwidth per SG decreases. However, in the proposed DSG scheme, the LGW dynamically changes N according to J and K using Table.1 and the boundary of P_{out} . Thus, the results of RSNs with $N=5$ are better than those of the proposed DSG scheme since in the proposed DSG scheme, the LGW increases N to guarantee the outage performance that is less than the boundary of P_{out} for SUEs.

Fig. 6 describes the results of $C_{Building}$ as the number of SUEs increases with different N . The results of RSNs increase as K increases in both 3x3 and 5x5 grid pattern models. However, in the proposed DSG scheme, the results of the 5x5 grid pattern model increase slowly while those of

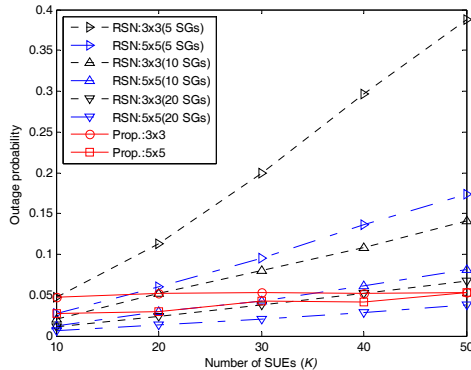


(Figure 7) Outage probability

the 3×3 grid pattern model are almost the same as K increases. This is because the proposed DSG scheme changes N to guarantee the outage performance that is less than the boundary of P_{out} .

Fig. 7 describes the results of P_{out} as the number of SUEs increases with different N . the results of RSNs increase greatly when N is 5 and 10 for the 3×3 grid pattern model and 5 for the 5×5 grid pattern model as K increases. This is because that the number of SUEs that receive no SGs from the serving SAPs increases as K increases. Therefore, the RSN models are difficult to be used as K increases even though the RSN has better performance than the proposed DSG scheme for the capacity as shown in Fig. 5 and 6. On the other hand, the results of the proposed DSG scheme are always less than the boundary of P_{out} in both the 3×3 and 5×5 grid pattern models.

5. Conclusion

In this paper, we proposed a novel DSG scheme using LGWs to maximize system capacity considering intended proper outage probability for the DL of ESNs. In the proposed DSG scheme, a LGW which is installed in a building dynamically changed the number of SGs for SAPs according to the number of SUEs per floor. Simulation results showed that the proposed DSG scheme is appropriate for ESNs compared to the RSNs in terms of the system capacity and outage probability. Further, we found that the

number of optimal SGs and the amount of appropriate bandwidth for each SAP in the proposed DSG scheme. For the future work, we plan to study an enhanced DSG scheme using optimal channel allocation with frequency reuse to reduce interference from adjacent SAPs for ESNs.

Reference

- [1] Cisco Visual Networking Index: Global Mobile Data Traffic Forecast Update, 2016 - 2021, White paper, CISCO, 2017.
<https://www.cisco.com/c/en/us/solutions/collateral/service-provider/visual-networking-index-vni/mobile-white-paper-c11-520862.html>
- [2] A. d. I. Fuente, R. P. Leal, A. G. Armada, "New Technologies and Trends for Next Generation Mobile Broadcasting Services," IEEE Communications Magazine, Vol. 54, No. 11, pp.217-223, 2016.
<https://doi.org/10.1109/MCOM.2016.1600216RP>
- [3] T. Nakamura, S. Nagata, A. Benjebbour, Y. Kishiyama, T. Hai, S. Xiaodong, Y. Ning, L. Nan, "Trends in small cell enhancements in LTE advanced," IEEE Communications Magazine, Vol. 51, No. 2, pp.98-105, 2013.
<https://doi.org/10.1109/MCOM.2013.6461192>
- [4] W. A. M. Weijermars, "Analysis of urban traffic patterns using clustering," Ph.D. dissertation, Univ. Twente, Enschede, The Netherlands, 2007.
https://research.utwente.nl/files/6069766/thesis_Weijermars.pdf
- [5] V. Chandrasekhar, J.G. Andrews, and A. Gatherer, "Femtocell Networks: A Survey," IEEE Communication Magazine, Vol. 46, No. 9, pp.59-67, 2008.
<https://doi.org/10.1109/MCOM.2008.4623708>
- [6] F.A. Zdarsky, A. Maeder, S. Al-Sabea, S. Schmid, "Localization of Data and Control Plane Traffic in Enterprise Femtocell Networks," VTC Spring 2011, pp.1-5, 2011.
<https://doi.org/10.1109/VETECS.2011.5956622>
- [7] N. Zhao, X. Liu, F. R. Yu, M. Li, V. C. M. Leung, "Communications, caching, and computing oriented small cell networks with interference alignment," IEEE

- Communications Magazine, Vol. 54, No. 9, pp.29-35, 2016.
<https://doi.org/10.1109/MCOM.2016.7565184>
- [8] S. Fortes, A. Aguilar-García, R. Barco, F. B. Barba, J. A. Fernández-luque; A. Fernández-Durán, “Management architecture for location-aware self-organizing LTE/LTE-a small cell networks,” IEEE Communications Magazine, Vol. 53, No. 1, pp.294-302, 2015.
<https://doi.org/10.1109/MCOM.2015.7010548>
- [9] D. Bojic, E. Sasaki, N. Cvijetic, T. Wang, J. Kuno, J. Lessmann, S. Schmid, H. Ishii, S. Nakamura, “Advanced wireless and optical technologies for small-cell mobile backhaul with dynamic software-defined management,” IEEE Communications Magazine, Vol. 51, No. 9, pp.86-93, 2013.
<https://doi.org/10.1109/MCOM.2013.6588655>
- [10] 3GPP TS 22.220, Service Requirements for Home NodeB (HNB) and Home eNodeB (HeNB), 2009.
<http://www.tech-invite.com/3m22/tinv-3gpp-22-220.html>
- [11] Small-Cell Forum, <http://www.smallcellforum.org>.
- [12] A. Prasad, O. Tirkkonen, P. Lundén, O. N. C. Yilmaz, L. Dalsgaard, C. Wijting, “Energy-efficient inter-frequency small cell discovery techniques for LTE-advanced heterogeneous network deployments,” IEEE Communications Magazine, Vol. 51, No. 5, pp.72-81, 2013.
<https://doi.org/10.1109/MCOM.2013.6515049>
- [13] X. Ge, J. Yang, H. Gharavi, Y. Sun, “Energy Efficiency Challenges of 5G Small Cell Networks,” IEEE Communications Magazine, Vol. 55, No. 5, pp.184-191, 2017.
<https://doi.org/10.1109/MCOM.2017.1600788>
- [14] Y. Mao, Y. Luo, J. Zhang, K. B. Letaief, “Energy harvesting small cell networks: feasibility, deployment, and operation,” IEEE Communications Magazine, Vol. 53, No. 6, pp.94-101, 2015.
<https://doi.org/10.1109/MCOM.2015.7120023>
- [15] J. M. R. Aviles, S. Luna-Ramirez, M. Toril, F. Ruiz, I. de la Bandera-Cascales, P. Munoz-Luengo, “Analysis of load sharing techniques in enterprise LTE femtocells,” WiAd 2011, pp.195-200, 2011.
<https://doi.org/10.1109/WiAd.2011.5983310>
- [16] G. Cao, D. Yang, R. An, X. Ye, R. Zheng, X. Zhang, “An adaptive sub-band allocation scheme for dense femtocell environment,” WCNC 2011, pp.102-107, 2011.
<https://doi.org/10.1109/WCNC.2011.5779114>
- [17] 3GPP TSG-RAN WG 4, R4-092042, Simulation assumptions and parameters for FDD HeNB RF requirements, 2009.
http://www.etsi.org/deliver/etsi_tr/136900_136999/136921/09.00.00_60/tr_136921v090000p.pdf
- [18] Y. Shi, A. B. MacKenzie, L. A. DaSilva, “On Resource Reuse for Cellular Networks with Femto- and Macrocell Coexistence,” IEEE GLOBECOM 2010, pp.1-6, 2011.
<https://doi.org/10.1109/GLOCOM.2010.5683443>

● 저 자 소 개 ●

김 세 진(Se-Jin Kim)

2004년 조선대학교 전산학과(이학사)

2006년 고려대학교 대학원 전산학과(이학석사)

2010년 고려대학교 대학원 전산학과(이학박사)

2015년~현재 조선대학교 컴퓨터통계학과 교수

관심분야 : 정보통신, 이동통신, Software Defined Network, 사물인터넷 etc.

E-mail : sjkim@chosun.ac.kr

